ARTICLE

The Preparation and Properties of Starch Based Shape Memory Hydrogel

Yangling Li[1], Zhengrong Li[1], Hui Yu[1], Gang Huang[1], Xiaopeng Pei[2], Kun Xu[2,*], Pixin Wang[2] and Ying Tan[3,*]

[1]School of Textile Materials and Engineering, Wuyi University, Jiangmen, 529000, China

[2]Key Laboratory of Polymer Ecomaterials, Changchun Institute of Applied Chemistry, Chinese Academy of Science, Changchun, 130022, China

[3]Wenzhou Institute, University of Chinese Academy of Sciences, Wenzhou, 325001, China

*Corresponding Authors: Kun Xu. Email: xukun@ciac.ac.cn; Ying Tan. Email: tanying@ciac.ac.cn

ABSTRACT

In this work, the –catechol and –thiol modified starch was prepared by the esterification and amino condensation reaction, then a fully starch based hydrogel was prepared via the thiol-catechol Michael addition reaction. The starch hydrogel gained shape memory behaviors by coordinate with Fe^{3+} ions at alkaline condition. ^{1}H-NMR had been used to character the structure of the starch derivatives and its character peaks. The hydrogel's modulus had also been measured before and after coordinating with Fe^{3+} ions in linear area and the result showed that both the hydrogel's storage modulus and loss modulus kept constant in linear area from 0.1 rad/s to 100 rad/s, which demonstrated a good network was formed inside the hydrogel. Furthermore, the shape memory behaviors had been tested by changing the pH value in solution. The result showed that the hydrogel can keep its temporary shape in high pH condition and recover to its original state after the shaped hydrogel immersed into acidic solution. This hydrogel might have great application prospects in the field of biomedical and engineering.

KEYWORDS

Starch; thiol-catechol Michael addition reaction; shape memory

1 Introduction

Shape-memory polymers (SMPs) which can retain two or three shapes are featured by the ability to return from a deformed state (temporary shape) to their original shape (permanent) induced by an external stimulus, such as pH, light, electric or magnetic field, solution and temperature [1–6]. As polymeric material, SMPs can be used in various industrial application (e.g., adaptive grip, automobile fenders and auto-choke element for engines) and medical applications (e.g., glaucoma shunts, intravenous cannula, self-adjusting orthodontic and intraocular lenses). Generally, SMPs contained thermoplastic polymeric materials, thermoset polymeric materials and hydrogels. Among them, the shape memory hydrogels (SMHs) had attracted more and more attention because of its unique properties such as flexibility, significant water content, responsive to specific molecules and small molecule diffusion [7–9]. For example, Wu's group had reported a shape memory hydrogel by incorporating gold nanorods (AuNRs) into the glassy gel matrix of poly(methacrylic acid-co-methacrylamide) without compromising the

excellent mechanical properties, where the near-infrared light could control this hydrogel's shape memory behaviors [10]. Zhang's group reported a hierarchically macro-micro-nanoporous structure's hydrogel constructs which can readily recover to their original shapes, and sustain high cell viability, proliferation, spreading, and differentiation after compression and injection [11]. David Diaz Diaz'g group reported a new series shape memory membranes composed of trialkyne deribatives of glycerol ethoxylate and bisphenol A diazide (BA-diazide) or diazide-terminated PEG600 monomer via a Cu(I)-catalyzed photoclick reaction. These hydrogel exhibit a reversible shape-memory effect in response to temperature through a defined phase transition [12]. Recently, the hot topic for the SMHs was mainly in supra-molecular interactions, host-guest interaction, micellar copolymerizaion, metal ions and phosphate, imidazole-zinc ion coordination and reversible phenylboronic acid-diol ester bonds [13–20].

Injectable hydrogels can translate its condition immediately from sol to gel. It is preferable for biomedical applications because they can be deployed by injection instead of surgical implantation. Based on different non-covalent and covalent interaction, lots of injectable SMHs hydrogel has been synthesized containing dual- or triple- shape memory effect triggered by pH, light, thermal, sugar, magnetic or salt [21–24]. For example, Gao's group reported a dual physically cross-linked shape memory hydrogel sensor via blending poly vinyl alcohol (PVA), cationic chitosan and grapheme oxide in water and glycerol, and this hydrogel can be used as a thermo-responsive shape memory sensor by virtue of orientation of PVA molecular chains under force and disorientation after heating [25]. Shi's group reported an injectable composite hydrogel based on a modified gelatin matrix integrated with shape-memory polymer fibers, where the gelatin matrix creates a local microenvironment for cell assembly and acts as a lubricant during injection through a fine catheter and shape memory fiber scaffolds are able to recover to maintain the microstructures even after dramatic deformation from injection operation, providing the necessary support and guidance for motor neuron differentiation [26]. In addition, in consideration of the practical application of SMHs in biomedical field, the introducing of natural components in such system is of interesting due to their biodegradability, biocompatibility, and sustainable ability [27–33].

Starch is a natural polysaccharide that has been widely investigated for many years in the biomedical field. We have shown recently that starch-based injectable hydrogel with well mechanical strength can be fabricated through a Schiff-base reaction and thiol-ene click reaction [34,35]. Here, a full starch based injectable SMHs is synthesized via the Thiol-catechol Michael Addition reaction. Dopamine and thiol group is separately grafted into the starch macromolecular backbone. And the injectable hydrogel formed by simply mixing the starch-dopamine (St-DA) and starch-catechol (St-CS) solution. The obtained hydrogel presents shape memory behaviors by coordinate with Fe^{3+} ions at alkaline condition. Moreover, its mechanical properties and shape memory behaviors ware also investigated in detail and this shape memory hydrogel might find applications in the biomedical and engineering fields [36,37].

2 Experimental

2.1 Materials

Corn starch purchased from Dacheng Corn Development Co., Ltd. (China). N-Hydroxysuccinimide (NHS), Succinic anhydride, Ethylenediaminetetraacetic acid (EDTA) and 1-(3-Dimethylaminopropyl)-3-ethylcarbodiimide hydrochloride (EDC) were purchased from Aladdin Chemistry Co., Ltd., Shanghai, China, Dopamine hydrochloride and L-Cysteine hydrochloride was achieved from Alfa Aesar Co., Ltd., Shanghai, China, All the other chemicals were obtained from Beijing Chemical Reagent and used as received.

2.2 Preparation of St-COOH

This step was manipulated as follow [35]: The starch (6.52 g) was put into 100 ml DMSO at 70°C. When the solution became clear, the temperature was adjusted to 60°C. Ten minutes later, imidazole (5.44 g), to be

used as catalyst and provide a good alkaline environment, and succinic anhydride (2.40 g), to be used as esterifying agent, were added and kept for 2 h. After that, the solution was kept for 24 h at room temperature and then was poured into 500 ml isopropanol solution. The precipitate was collected after washed for several times and dried in at 45°C in vacuum oven.

The degree of –COOH's substitution was about 0.67 (obtained by area integration from ^{1}H-NMR spectra). ^{1}H-NMR (D$_2$O): δ = 4.84–5.70 ppm, 3.20–4.65 ppm (AGU, H; where AGU represents the anhydroglucose unit in starch and the H represents the hydrogen atom), δ = 2.45–2.67 ppm (succinic H).

2.3 Preparation of the St-CS

St-CS's synthesis was as follow [35]: St-COOH (2.00 g) was added at a concentration of 25 mg/ml in PBS (0.1 M) solutions at 8°C. Then NHS (1.42 g) and EDC (2.40 g) were added under stirring; after that, 2.18 g L-Cysteine hydrochloride was put (COOH/L-Cysteine hydrochloride approximately 1/2 (mol/mol)) and the solution's pH kept 5.5 by dropping 1 M NaOH solution. After 12 hours, the crude product dialyzed at pH = 5.0 for three times against 0.01 M PBS solutions and then for other three times against distilled water. Finally, the polymers were collected after freeze-drying.

The degree of St-CS's substitution was about 0.16 (obtained by area integration from ^{1}H-NMR spectra). ^{1}H-NMR (D$_2$O): δ = 3.10–3.22 ppm, 4.85–5.70 ppm (AGU H); δ = 3.10–3.22 ppm (cysteine methylene H); δ = 3.00–2.3 ppm (succinic H).

2.4 Preparation of the St-DA

St-DA was prepared as follow: St-COOH (2.00 g) was added at a concentration of 25 mg/ml in PBS (0.1 M) solutions at 8°C. Then NHS (1.42 g) and EDC (2.40 g) were added under stirring; after that, 2.18 g Dopamine hydrochloride was put (COOH/ Dopamine hydrochloride approximately 1/2 (mol/mol)) and the solution's pH kept 5.5 by dropping 1 M NaOH solution. After 12 h, the crude product dialyzed at pH = 5.0 for three times against 0.01 M PBS solutions and then for other three times against distilled water. Finally, the polymers were collected after freeze-drying.

The degree of St-DA's substitution was about 0.19 (obtained by area integration from ^{1}H-NMR spectra). ^{1}H-NMR (D$_2$O): δ = 2.13–3.00 ppm (succinic H); δ = 5.68–4.94 ppm, 3.37–4.46 ppm (AGU H); δ = 5.68–7.55 ppm (benzene H).

2.5 Preparation of Starch Based Hydrogel

Typically, 20wt% St-DA Tris-HCL buffer solutions (10 mM, pH = 8.5) and 20 wt% St-CS Tris-HCL buffer solutions (10 mM, pH = 8.5) were mixing together through a co-extrusion needle to form hydrogel. Then we used inverted method to confirm the formation of the hydrogel and the gelation time.

2.6 Characterization

The degree of substitution of St-COOH, St-CS and St-DA were determined by ^{1}H-NMR where the deuterium oxide was used as solvent. The modulus of the hydrogel was tested by rheometer (Ta Rheometer Discovery HR3) at 25°C. Firstly, the strain was changing from 0.1% to 100% to select the linear viscoelastic region (oscillation model) at fixed frequencies of 1 Hz. Then, the hydrogel's modulus was tested by changing the frequency from 100 rad/s to 0.01 rad/s at linear viscoelastic region.

2.7 Evaluation of Shape Memory Performance

The shape memory behaviors of the hydrogels were evaluated at room temperature. A straight columned of hydrogel (30 mm × 1 mm) was immersed into 0.05 M FeCl$_3$ Tris-HCL solution (10 mM, pH ≈ 11.0) and bent it into a V-form shape for 3 h to fix the temporary "V" shape. The shape recovery of the hydrogel was

finally investigated through the immersing of the hydrogel into Tris-HCL buffer solutions (10 mM, pH = 11), Tris-HCL buffer solutions (10 mM, pH = 2.0) and 0.1 M EDTA solutions, respectively.

2.8 Evaluation of Shape Memory Cycle

The quantitative shape memory cycle was determined according to the reported method. The shape fixity ratio (R_f) and shape recovery ratio (R_r) were defined by the following equation:

$$R_f = {}^{\theta_t}/_{\theta_d} \times 100\% \tag{1}$$

$$R_r = (\theta_d - \theta_f)/\theta_d \times 100\% \tag{2}$$

where θ_d is the given angle, θ_t is the temporarily fixed angle, and θ_f is the finished angle.

3 Results and Discussion

3.1 Synthesis of St-CS and St-DA

In our approach, the succinic anhydride was successfully grafted to the starch backbone using imidazole as catalyst agent, offering carboxyl groups to the starch's backbone (Fig. 1). As shown in Fig. 2, ^{1}H-NMR showed resonance characteristic of St-COOH signals at δ = 2.67–2.45 ppm (a, b) attributable to the methylene protons of succinic anhydride, indicating the succinic groups had grafted into the starch backbone successfully and the imidazole was an effective catalyst agent. The degree of substitution of succinic anhydride (DS, defined as the number of succinic anhydride per glucose unit) could be estimated by comparing the integrals area of signal at δ = 2.67–2.45 ppm and δ = 5.70–4.84 ppm, 4.65–3.20 ppm (AGU H) which was calculated to ≈0.67. It was noted that if the degree of substitution was beyond 0.67, the yield of the product would reduce significantly. This phenomenon can be explained as follows: The -COOH group can change starch's solubility, especially when the –COOH's degree of substitution beyond 0.67, the St-COOH's solubility increased in isopropanol.
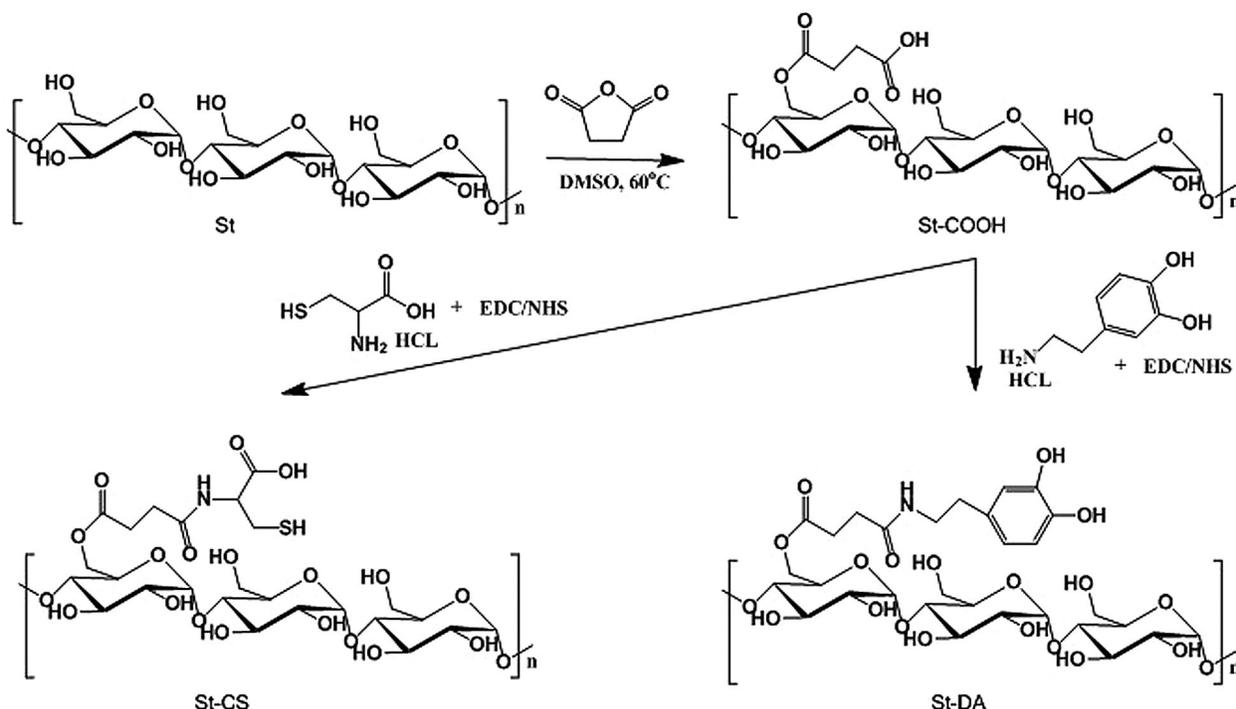

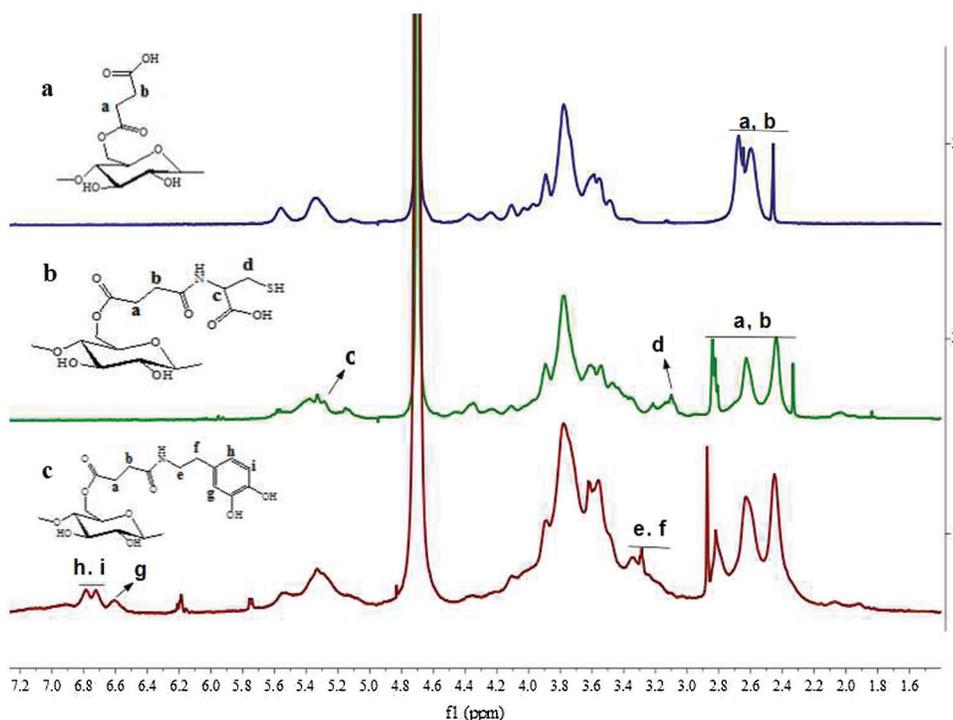**Figure 1:** The process to prepare St-CS and St-DA

Figure 2: The ^{1}H-NMR (D$_2$O) of St-COOH (a), St-CS (b) and St-DA (c)

Furthermore, the carboxyl groups were reacted with L-cysteine hydrochloride to gain the thiol groups using EDC/NHS as coupling agent to form St-CS. The signals appeared at δ = 3.22–3.10 ppm (c, d) might be the character peaks for L-cysteine (Fig. 2). The degree of substitution of L-cysteine was about 0.16 calculated by comparing the integrals area of signal δ = 3.22–3.10 ppm and δ = 5.70–4.85 ppm, 4.65–3.20 ppm. On the other side, the dopamine hydrochloride was also reacted with carboxyl groups as mentioned above. As showed in Fig. 2, the signals, appeared at δ = 7.55–5.68 ppm, were attributed to character peaks for protons of the benzene groups. It demonstrated that the dopamine groups have been successfully introduced to the starch backbone. The substitution degree was also calculated by comparing the integrals area of δ = 7.55–5.68 ppm (benzene H) and δ = 5.68–4.94 ppm, 4.46–3.37 ppm (AGU H) which was calculated to ≈0.19.

3.2 Preparation of the Hydrogel and its Derivation

The hydrogel was formed by simple mix St-CS and St-DA in Tris-HCl solutions (10 mM, pH = 8.5) through a co-extrusion needle. As is reported, the catechol structure of the dopamine could become quinone structure at alkaline condition [38,39]. And the quinone groups could react with thiol or amine groups via Michael addition reaction. Herein, when the St-CS and St-DA were mix together at alkaline condition, the catechol groups in St-DA would react with thiol groups in St-CS via Michael addition reaction resulting in the formation of the hydrogel (Fig. 3). Here a series of hydrogel was prepared by adjusting the molar ratio between the St-CS and the St-DA, and these hydrogel's gelation time had been measured by inverted method. The data was collected in Tab. 1 and the result showed that the gelation time become longer from 3 min to 20 min when the St-DA's molar reduced from 0.2 mmol to 0.02 mmol while kept the St-CS's molar as 0.20 mmol. As a comparison, the pure St-DA solution and pure St-CS solution had also been investigated to confirm if they could form hydrogel. The result demonstrated pure St-DA cannot form the hydrogel ever for a long time. On the other side, for St-CS, it can form hydrogel

due to the air oxidation of free SH groups to S-S bridges among the thiols groups [40,41], but for a very long time, almost 48 h. Here, we took Gel-C1D1 as target sample to investigate the property of the hydrogel because of its short gelation time.
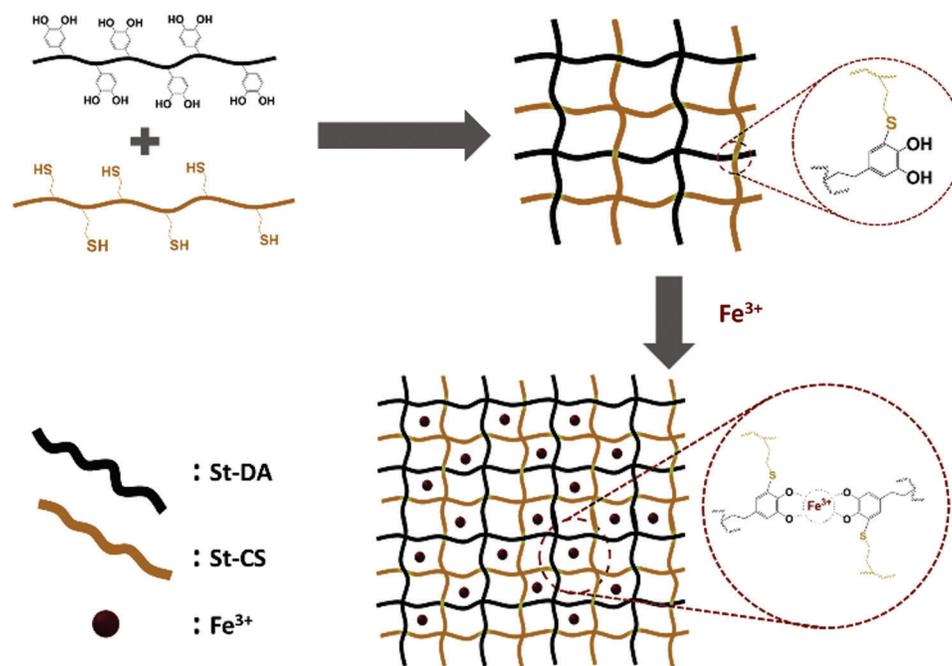

Figure 3: The process to prepare the hydrogel with or without Fe^{3+} ions

Table 1: The component of the hydrogel and its gelation time

Samples	St-CS (mmol)	St-DA (mmol)	Product	Gelation time (min)
Gel-C1D1	0.20	0.20	Gel	3
Gel-C1D0.8	0.20	0.16	Gel	5
Gel-C1D0.4	0.20	0.08	Gel	10
Gel-C1D0.2	0.20	0.04	Gel	20
Gel-C1D0	0.20	0.00	Gel	48h
Gel-C0D1	0.00	0.20	Sol	–

In addition, the Gel-C1D1 was immersed into 0.05 M $FeCl_3$ Tris-HCL solutions (10 mM, pH ≈ 11) to form the second network between Fe^{3+} ions and catechol groups via metal-coordination interaction as is shown in Fig. 3. We called it as Gel-C1D1&Fe. It is worth noting that the first network was formed via covalent coupling in alkaline condition. The pH value in 0.05 M $FeCl_3$ Tris-HCL solutions (10 mM) was about 11, in this case, the tris-complex was the major component in the second network. Many groups had reported that Fe^{3+} ions could coordinate with catechol to form mono-complex, bis-complex and tris-complex at different pH condition [42]. The relationship among these complexes was significantly depending on the pH condition. Generally speaking, the mono-, bis-, and tris-complex were found to

dominate in solutions in pH ranges 1–5, 5–10.8 and 10.8–12, respectively [43]. So based on that description, it could be speculated that the major component in the second network was tris-complex.

3.3 The Mechanical Property

The hydrogel's mechanical property was investigated by rheometer. As shown in Fig. 4a, when the frequency was fixed at 1 Hz, the Gel-C1D1 can keep its network structure before the strain got 45%. It demonstrated that the Gel-C1D1 can bear about 45% strain without yielding. In addition, if Gel-C1D1 reacted with Fe^{3+} via the chelate effect to form another network, the hydrogel will become rigid and its strength will increase accordingly. It can be seen from Fig. 4b, both the storage and loss modulus of the hydrogel, Gel-C1D1&Fe, became larger compared with the original state. The Gel-C1D1&Fe's storage modulus has increased from 2000 Pa to 9000 Pa, which is an increase by 4.5 times. On the other side, the Gel-C1D1&Fe's maximum strain is getting smaller, about 12%. So, it can be concluded from Fig. 4a that the Gel-C1D1 could react with Fe^{3+} via metal-catechol interaction to form the second network to enhance the hydrogel's mechanical property. Furthermore, both hydrogel's modulus had been tested in linear viscoelastic region (in oscillation). As shown in Fig. 4b, both hydrogel's modulus preformed almost constant in the whole frequency area. It further confirmed that a uniformed network had formed inside the hydrogel, even treated with Fe^{3+} irons.
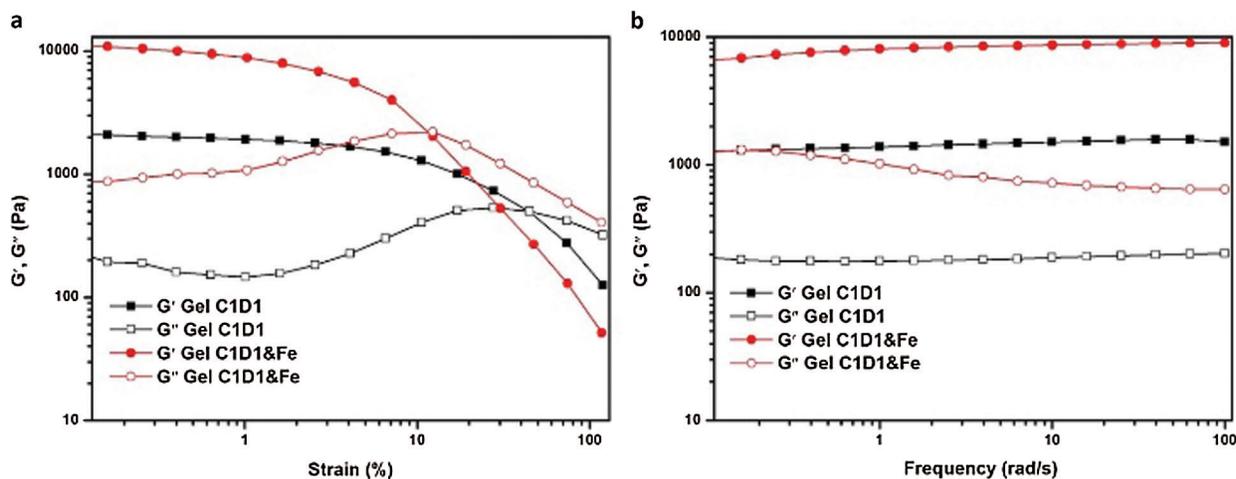

Figure 4: The Gel-C1D1 and Gel-C1D1&Fe's stress-strain and stress-frequency curve

3.4 Shape Memory Performance

In our system, the covalent crosslink between thiol and quinone formed the permanent network meanwhile the complexation between Fe^{3+} and catechol groups formed the temporary network. Because of the reversibility of the Fe^{3+}-catechol complex, the hydrogel could obtain pH responsive ability. Here, we immersed the Gel-C1D1 into 0.05 M $FeCl_3$ Tris-HCL solutions (10 mM, pH ≈ 11) with a fixed "V" shape to get the temporary shape base on the Fe^{3+}-catechol tris-complex interaction. After the shape was fixed, the hydrogel, Gel-C1D1&Fe, was washed by distilled water several times and then put into pH = 2.0 Tris-HCL buffer solution (10 mM) and pH = 11 Tris-HCL buffer solution (10 mM) respectively, to observe the shape recover behaviors. As seen in Fig. 5a, the Gel-C1D1&Fe's recover behaviors with "V" shape was performed to study the shape recover behaviors.
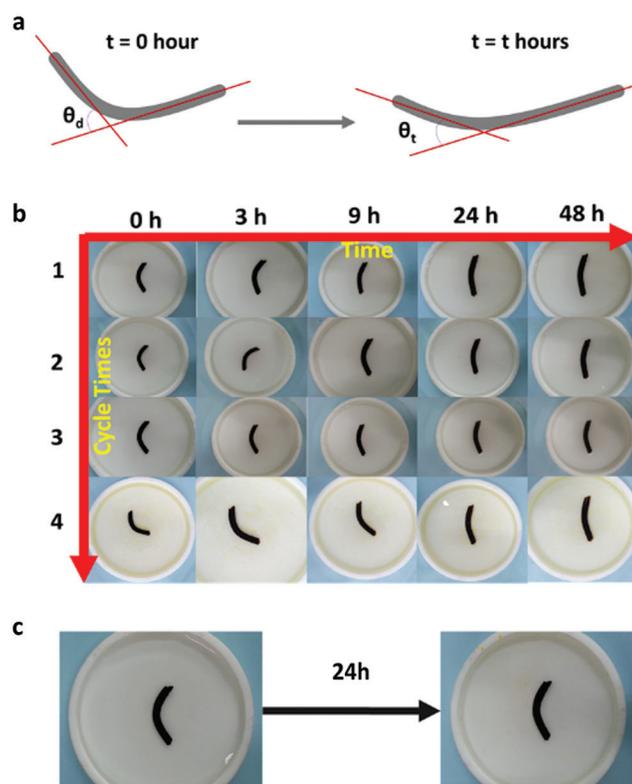
Figure 5: a) The angle change at different time; b) The Gel-C1D1&Fe's cycle shape recovery behaviours at different time in pH = 2.0 Tris-HCL buffer solution; c) The Gel-C1D1&Fe's shape recovery behaviours after 24 h in pH = 11 Tris-HCL buffer solution

Then we used protractor to measure the angle change at different time interval and calculated the shape fixing efficiency. The data was listed in Tab. 2. As seen in Fig. 5b, the Gel-C1D1&Fe's shape was changing from "V" shape to "-" shape slowly. After 24 h later, the shape recovery got equilibrium and then even if the time was extended to 48 hours, there was no obvious changing of Gel-C1D1&Fe's shape. The Gel-C1D1&Fe's shape recovery behaviors had been totally tested four times to calculate the shape fixing efficiency and shape recover ratio. As seen in Tab. 2, there were almost no change for the result of the Gel-C1D1&Fe's shape recover ratio, that confirmed the hydrogel own the shape recover ability in acidic condition. Further, the shape recover ability in alkaline condition was also tested in Tris-HCL buffer solution (10 mM, pH = 11) for comparison. The result showed that there was almost no changing for the Gel-C1D1&Fe's shape in Fig. 4c. So, the Gel-C1D1&Fe could not get shape recover ability in alkaline condition.

Table 2: The Gel-C1D1&Fe's shape fixing efficiency and shape recovery ratio

Cycle times	Rf/%				
	3 h	9 h	24 h	48 h	Rr/%
1	84	44	28	26	74%
2	85	62	27	27	73%
3	75	58	30	28	72%
4	81	55	32	31	69%

The mechanism of the shape memory behaviors of the Gel-C1D1&Fe was shown in Fig. 6, exhibiting that the tris-complex account for the majority of the hydrogel when the pH value was beyond 10.8, the bis-complex explained for the majority of the hydrogel when the pH value was between 5.0 and 10.8, and the mono- complex accounted for the majority of the hydrogel when the pH value was ranging from 1 to 5. So, in this case, when the hydrogel was fixed at "V" shape at high pH condition (pH = 11), tris- complex were the driving force to form temporary shape. When the "V" shape hydrogel was immersed into alkaline condition (pH = 11), there was no shape changing because of no bonds had been broken in that condition. On the other side, if the hydrogel was immersed into acidic pH condition (e.g., pH = 2.0), under this circumstances, the bond interaction between the Fe^{3+} and catechol groups would change from tris-complex to mono-complex, resulting the shape changed from "V" shape to "-" shape.
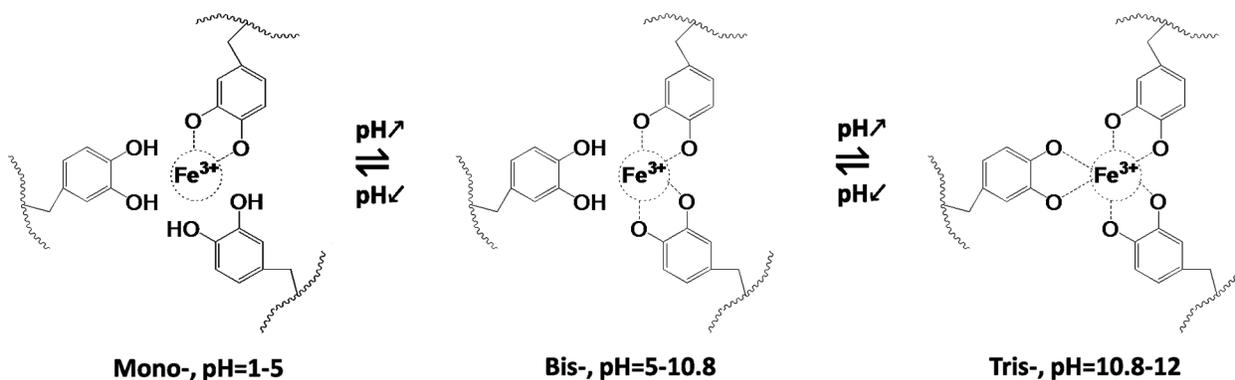

Figure 6: The relationship between Fe^{3+} and catechol at different pH conditions

Here, it should be noted that the Gel-C1D1&Fe's shape could not recover completely due to the existing of mono-complex. To eliminate the influence of the mono- complex and get fully shape recover ratio, the EDTA was introduced into the system at the last stage. Because the EDTA can competitive with catechol groups to form chelation with Fe^{3+} ions, the $K_f = 1.7 \times 10^{24}$ ([Fe(EDTA)]⁻). As showed in Fig. 7, the hydrogel could recover to its original shape within 2 h with the help of 0.1 M EDTA solution.
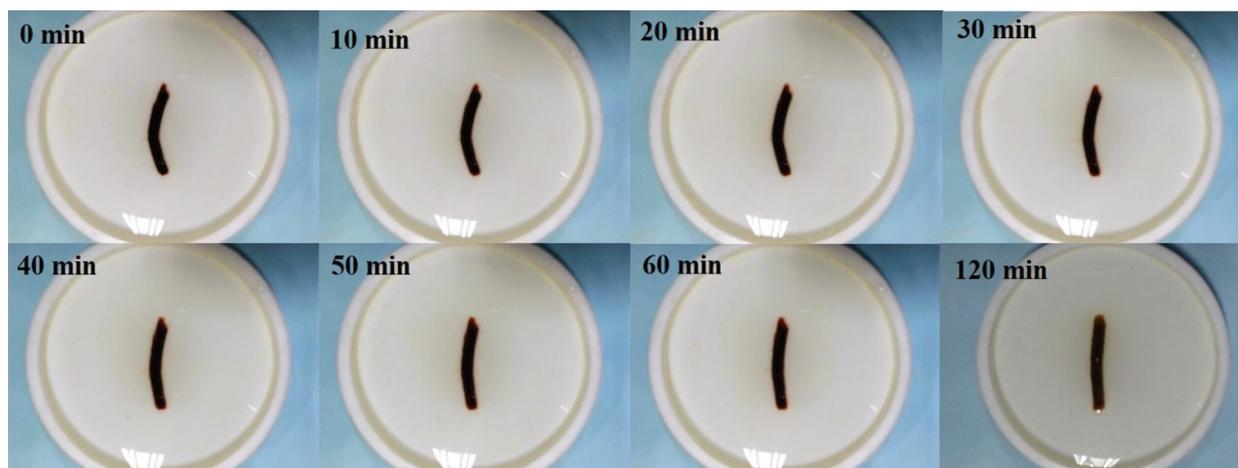

Figure 7: The shape recovery behaviors of mono-complex C1D1&Fe hydrogel in 0.1 M EDTA solution at different time

4 Conclusions

A fully starch base shape memory hydrogel was prepared via the thiol-catechol Michael addition reaction. The hydrogel can keep its temporary shape at alkaline condition for a long time, and change its shape to original state if the pH switched to acidic condition. This shape recover behaviours could repeat several times while there was almost no changing for the shape recover ratio. The starch hydrogel could not recover completely because of the mono-complex interaction between the Fe^{3+} and catechol in acidic condition. But the EDTA can make the hydrogel's shape recover completely due to the strong interaction between the Fe^{3+} and EDTA. It demonstrated that the interaction between Fe^{3+}-catechol was a weak bond compared with the interaction between Fe^{3+} and EDTA. This method might provide a new candidate for application in biomedical and engineering fields.

Conflicts of Interest: The authors declare that they have no conflicts of interest to report regarding the present study.

References

1. Guo, W., Lu, C. H., Orbach, R., Wang, F., Qi, X. J. et al. (2015). pH-stimulated DNA hydrogels exhibiting shape-memory properties. *Advanced Materials, 27(1),* 73–78. DOI 10.1002/adma.201403702.

2. Lendlein, A., Jiang, H., Jünger, O., Langer, R. (2005). Light-induced shape-memory polymers. *Nature, 434(7035),* 879–882. DOI 10.1038/nature03496.

3. Deng, J., Chang, Z., Zhao, T., Ding, X., Sun, J. et al. (2016). Electric field induced reversible phase transition in Li doped phosphorene: Shape memory effect and superelasticity. *Journal of the American Chemistry Society, 138(14),* 4772–4778. DOI 10.1021/jacs.5b13274.

4. Liu, Y., Xu, K., Chang, Q., Darabi, M. A., Lin, B. et al. (2016). Highly flexible and resilient elastin hybrid cryogels with shape memory, injectability, conductivity, and magnetic responsive properties. *Advanced Materials, 28(35),* 7758–7767. DOI 10.1002/adma.201601066.

5. Cui, Y., Tan, M., Zhu, A., Guo, M. (2014). Mechanically strong and stretchable PEG-based supramolecular hydrogel with water-responsive shape-memory property. *Journal of Materials Chemistry B, 2(20),* 2978–2982. DOI 10.1039/C4TB00315B.

6. Jeon, S., Hauser, A., Hayward, R. (2017). Shape-morphing materials from stimuli-responsive hydrogel hybrids. *Accounts of Chemical Research, 2(50),* 161–169. DOI 10.1021/acs.accounts.6b00570.

7. Zhang, X., Cai, J., Liu, W., Qiu, X. (2019). Synthesis of strong and highly stretchable, electrically conductive hydrogel with multiple stimuli responsive shape memory behavior. *Polymer, 188,* 122–147. DOI 10.1016/j.polymer.2019.122147.

8. Koga, T., Tomimori, K., Higashi, N. (2020). Transparent, high-strength, and shape memory hydrogels from thermo-responsive amino acid-derived vinyl polymer networks. *Macromolecular Rapid Communications, 41(7),* 1900650. DOI 10.1002/marc.201900650.

9. Cera, L., Gonzalez, G. M., Liu, Q., Choi, S., Parker, K. K. (2020). A bioinspired and hierarchically structured shape-memory material. *Nature Materials, 1–8,* DOI 10.1038/s41563–020-0789-2.

10. Dai, C. F., Du, C., Xue, Y., Zhang, X. N., Zheng, Q. (2019). Photo-directed morphing structures of nanocomposite shape memory hydrogel with high stiffness and toughness. *ACS Applied Materials & Interfaces, 11(46),* 43631–43640. DOI 10.1021/acsami.9b16894.

11. Ying, G., Jiang, N., Parra-Cantu, C., Tang, G., Zhang, J. et al. (2020). Bioprinted injectable hierarchically porous gelatin methacryloyl hydrogel constructs with shape-memory properties. *Advanced Functional Materials, 30(46),* 2003740. DOI 10.1002/adfm.202003740.

12. Maiti, B., Abramov, A., Franco, L., Puiggalí, J., Enshaei, H. et al (2020). Thermoresponsive shape-memory hydrogel actuators made by phototriggered click chemistry. *Advanced Functional Materials, 30(24),* 2001683. DOI 10.1002/adfm.202001683.

13. Meng, H., Xiao, P., Gu, J., Wen, X., Xu, J. et al. (2014). Self-healable macro-/microscopic shape memory hydrogels based on supramolecular interactions. *Chemical Communications, 50(82),* 12277–12280. DOI 10.1039/C4CC04760E.

14. Le, X., Lu, W., Zheng, J., Tong, D., Zhao, N. et al. (2016). Stretchable supramolecular hydrogels with triple shape memory effect. *Chemical Science, 7(11),* 6715–6720. DOI 10.1039/C6SC02354A.

15. Miyamae, K., Nakahata, M., Takashima, Y., Harada, A. (2015). Self-healing, expansion-contraction, and shape-memory properties of a preorganized supramolecular hydrogel through host-guest interactions. *Angewandte Chemie International Edition, 54(31),* 8984–8987. DOI 10.1002/anie.201502957.

16. Bilici, C., Okay, O. (2013). Shape memory hydrogels via micellar copolymerization of acrylic acid and n-Octadecyl acrylate in aqueous media. *Macromolecules, 46(8),* 3125–3131. DOI 10.1021/ma400494n.

17. Zhao, T., Tan, M., Cui, Y., Deng, C., Huang, H. et al. (2014). Reactive macromolecular micelle crosslinked highly elastic hydrogel with water-triggered shape-memory behaviour. *Polymer Chemistry, 5(17),* 4965–4973. DOI 10.1039/C4PY00554F.

18. Yasin, A., Li, H., Lu, Z., Rehman, S., Siddiq, M. et al. (2014). A shape memory hydrogel induced by the interactions between metal ions and phosphate. *Soft Matter, 10(7),* 972–977. DOI 10.1039/C3SM52666F.

19. Nan, W., Wang, W., Gao, H., Liu, W. (2013). Fabrication of a shape memory hydrogel based on imidazole–zinc ion coordination for potential cell-encapsulating tubular scaffold application. *Soft Matter, 9(1),* 132–137. DOI 10.1039/C2SM26918J.

20. Meng, H., Zheng, J., Wen, X., Cai, Z., Zhang, J. et al. (2015). pH- and sugar-induced shape memory hydrogel based on reversible phenylboronic Acid-Diol ester bonds. *Macromolecular Rapid Communications, 36(6),* 533–537. DOI 10.1002/marc.201400648.

21. Han, X. J., Dong, Z. Q., Fan, M. M., Liu, Y., Wang, Y. F. et al. (2012). pH-induced shape-memory polymers. *Macromolecular Rapid Communications, 33(12),* 1055–1060. DOI 10.1002/marc.201200153.

22. Feng, W., Zhou, W., Zhang, S., Fan, Y., Yasin, A. et al. (2015). UV-controlled shape memory hydrogels triggered by photoacid generator. *RSC Advances, 5(100),* 81784–81789. DOI 10.1039/C5RA14421C.

23. Hao, J., Weiss, R. (2013). Mechanically tough, thermally activated shape memory hydrogels. *ACS Macro Letters, 2(1),* 86–89. DOI 10.1021/mz3006389.

24. Gulyuz, U., Okay, O. (2014). Self-healing poly(acrylic acid) hydrogels with shape memory behavior of high mechanical strength. *Macromolecules, 47(19),* 6889–6899. DOI 10.1021/ma5015116.

25. Yang, T. Y., Wang, M., Jia, F., Ren, X. Y., Gao, G. H. (2020). Thermo-responsive shape memory sensors based on tough, remolding and anti-freezing hydrogels. *Journal of Materials Chemistry C, 8(7),* 2326–2335. DOI 10.1039/C9TC05804D.

26. Wang, C., Yue, H. B. (2018). Injectable nanoreinforced shape-memory hydrogel system for regenerating spinal cord tissue from traumatic injury. *ACS Applied Materials & Interfaces, 10(35),* 29299–29307. DOI 10.1021/acsami.8b08929.

27. Bencherif, S. A., Sands, R. W., Bhatta, D., Arany, P., Verbeke, C. S. et al. (2012). Injectable preformed scaffolds with shape-memory properties. *Proceedings of the National Academy of Sciences of the United States of America, 109(48),* 19590–19595. DOI 10.1073/pnas.1211516109.

28. Izawa, H., Kaneko, Y., Kadokawa, J. I. (2009). Unique gel of xanthan gum with ionic liquid and its conversion into high performance hydrogel. *Journal of Materials Chemistry, 19(38),* 6969–6972. DOI 10.1039/b916864h.

29. Yu, F., Cao, X., Du, J., Wang, G., Chen, X. (2015). Multifunctional hydrogel with good structure integrity, self-healing, and tissue-adhesive property formed by combining Diels–Alder click reaction and acylhydrazone bond. *ACS Applied Materials & Interfaces, 7(43),* 24023–24031. DOI 10.1021/acsami.5b06896.

30. Ren, H. W., Wang, L., Bao, H., Xia, Y. Y., Xu, D. et al. (2020). Improving the antibacterial property of chitosan hydrogel wound dressing with licorice polysaccharide. *Journal of Renewable Materials, 8(10),* 1343–1355. DOI 10.32604/jrm.2020.010903.

31. Thakur, S., Sharma, B., Verma, A., Chaudhary, J., Tamulevicius, S. (2018). Recent progress in sodium alginate based sustainable hydrogels for environmental applications. *Journal of Cleaner Production, 198,* 143–159. DOI 10.1016/j.jclepro.2018.06.259.

32. Burhan, A., Suleyman, K., Ahmet, U., Canbolat, G., Vijay, K. T. (2020). Chemistry, structures, and advanced applications of nanocomposites from biorenewable resources. *Chemical Reviews, 120(17),* 9304–9362. DOI 10.1021/acs.chemrev.9b00553.

33. Bhawna, S., Sourbh, T., Gcina, M., Prateek, Raju, K. G. et al. (2020). Titania modified gum tragacanth based hydrogel nanocomposite for water remediation. *Journal of Environmental Chemical Engineering, 9(1),* 104608. DOI 10.1016/j.jece.2020.104608.

34. Li, Y., Liu, C., Tan, Y., Xu, K., Lu, C. et al. (2014). In situ hydrogel constructed by starch-based nanoparticles via a Schiff base reaction. *Carbohydrate Polymers, 110(6),* 87–94. DOI 10.1016/j.carbpol.2014.03.058.

35. Li, Y., Tan, Y., Xu, K., Lu, C., Liang, X. et al. (2015). In situ crosslinkable hydrogels formed from modified starch and O-carboxymethyl chitosan. *RSC Advances, 5(38),* 30303–30309. DOI 10.1039/C4RA14984J.

36. Korde, J. M., Kandasubramanian, B. (2020). Naturally biomimicked smart shape memory hydrogels for biomedical functions. *Chemical Engineering Journal, 379,* 122430. DOI 10.1016/j.cej.2019.122430.

37. Delaey, J., Dubruel, P., van, S. (2020). Shape-memory polymers for biomedical applications. *Advanced Functional Materials., 30(44),* 1909047. DOI 10.1002/adfm.201909047.

38. Cencer, M., Liu, Y., Winter, A., Murley, M., Meng, H. et al. (2014). Effect of pH on the rate of curing and bioadhesive properties of dopamine functionalized poly(ethylene glycol) hydrogels. *Biomacromolecules, 15(8),* 2861–2869. DOI 10.1021/bm500701u.

39. Lee, Y. K., Lee, S. Y. (2014). A colorimetric alginate-catechol hydrogel suitable as a spreadable pH indicator. *Dyes and Pigments, 108(1),* 1–6. DOI 10.1016/j.dyepig.2014.04.014.

40. Palumbo, F. S., Pitarresi, G., Albanese, A., Calascibetta, F., Giammona, G. (2010). Self-assembling and auto-crosslinkable hyaluronic acid hydrogels with a fibrillar structure. *Acta Biomaterialia, 6(1),* 195–204. DOI 10.1016/j.actbio.2009.06.014.

41. Shu, X. Z., Liu, Y., Luo, Y., Roberts, M. C., Prestwich, G. D. (2002). Disulfide cross-linked hyaluronan hydrogels. *Biomacromolecules, 3(6),* 1304–1311. DOI 10.1021/bm025603c.

42. Holten-Andersen, N., Harrington, M. J., Birkedal, H., Lee, B. P., Messersmith, P. B. et al. (2011). pH-induced metal-ligand cross-links inspired by mussel yield self-healing polymer networks with near-covalent elastic moduli. *Proceedings of the National Academy of Sciences of the United States of America, 108(7),* 2651–2655. DOI 10.1073/pnas.1015862108.

43. Krogsgaard, M., Behrens, M. A., Pedersen, J. S., Birkedal, H. (2013). Self-healing Mussel-inspired multi-pH-responsive hydrogels. *Biomacromolecules, 14(2),* 297–301. DOI 10.1021/bm301844u.